Electronic Supplementary Material (ESI) for Journal of Materials Chemistry A.
This journal is © The Royal Society of Chemistry 2018

A Cobalt Sulfide Cluster-Based Catholyte for Aqueous Flow Battery Applications

Matthew B. Freeman, Le Wang, Daniel S. Jones and Christopher M. Bejger*

Department of Chemistry, University of North Carolina at Charlotte, 9201 University City Boulevard, Charlotte North Carolina 28223, USA.

Supporting Information

I. Synthetic Details

General Information

All reagents were purchased from commercial sources and used as is. The following was used from the commercial suppliers: cobalt (II) chloride (anhydrous) (Alfa Aesar, 99.9%), tetrakis(hydroxymethyl)phosphonium chloride (Aldrich, 80% in solution), formaldehyde (Aldrich, 37% in solution), hexamethylenetetramine (Aldrich, 99.9%), sodium sulfide nonahydrate (Acros Organic, 98%), phosphoric acid (Macron, 85% in solution), sodium chloride (Sigma Aldrich, 99.999%), methyl viologen hydrate (Acros Organics, 98%), sodium hydroxide (Macron, 99%), potassium hydroxide (Macron, Reagent Grade). 1,3,5-Triaza-7-phosphaadamantane (PTA) was synthesized according to a literature method reported by Donald J. Daigle.[1]

Solvents were bought from commercial suppliers and used without further purification. Acetone (Fisher), methanol (Macron) and 190 proof ethanol (Koptec) were degassed via sparging with nitrogen before use. All manipulations were performed under inert atmosphere using standard Schlenk techniques.

$Co_6S_8(PTA)_6$•4HCl (1)

$CoCl_2$ (0.259 g, 2 mmol) was stirred with PTA (0.628 g, 4 mmol) in 35 mL of sparged methanol at 45°C. The solution was allowed to stir for 1 h noting that the color changed from purple ($CoCl_2$ hydrate), to orange (after PTA addition), to green until a dark purple precipitate formed. Hydrogen sulfide was then generated in a separate flask by dripping 85% H_3PO_4 on to Na_2S•$9H_2O$ at 24 drops per minute. The hydrogen sulfide was allowed to purge through the needle and line connected to the flask before being bubbled into the hot methanol solution. The hydrogen sulfide was bubbled through for 1 h noting that the dark purple precipitate turned into a fine dark brown suspension. The excess H_2S was trapped in a caustic solution pH ~14 and neutralized with bleach. The reaction solution was stirred for 5 h and then filtered under inert conditions. The dark black solid was washed with acetone and the product collected was dissolved in a minimal amount of water and layered 1:3 with 190 proof ethanol inside a scintillation vial. The vial was allowed to sit until the layers fully mixed. This method yielded sharp, dark brown, single X-ray quality crystals (0.327 g, 48% average over five reactions). Note: crystals of **1** appear to be unstable when dried for extended periods of time under high vacuum. ^{1}H NMR (500 MHz, D_2O): δ 2.97 (s, 4H, NH), 2.84 (m, 18H, N-C**H₂**-N)*, 2.71 (m,18H, N-C**H₂**-N)*, 2.48 (m, 36H, P-C**H₂**-N). Elemental analysis for $C_{36}H_{76}Cl_4Co_6N_{18}P_6S_8$, Calculated: C 25.45, H 4.51, N 14.84, S 15.10, Cl 8.35. Found: C 24.94, H 4.49, N 14.15, S 13.38, Cl 8.70.

II. Measurements

Ultraviolet-visible Spectroscopy

UV-vis spectra were obtained on a Cary 300 UV-vis spectrophotometer with quartz cells (1 cm path length) with all solutions made using volumetric glassware and micropipettes. The samples were prepared under ambient conditions.

Electrochemical Measurements

All electrochemical measurements were obtained on a Gamry 1000E potentiostat and were recorded on Gamry Framework Software (Version 7.02). Analysis of the data was done using Gamry Echem Analyst (Version 7.02).

Static Electrochemical Measurements

For cyclic voltammetry and chronoamperometry, a three-electrode set up was used with a BASi glassy carbon working electrode, silver wire as the counter electrode, and a Ag/AgCl quasireference electrode.

Galvanostatic Half Cell Cyclic Charge Discharge

An Adam & Chittenden H cell (8 mL) was used with a Selemion AMV anion exchange membrane and sealed with a Viton rubber O-ring. Graphite felt electrodes (Fuel Cell Store) were cut and placed into an oven at 200 °C for 1 h before use. The graphite felt electrodes were submerged to have a surface area of (1 mm x 10 mm x 3mm). The half-cell was referenced versus Ag/AgCl quasireference electrode.

Galvanostatic Full Cell Cyclic Charge Discharge

An Adam & Chittenden H-cell (8 mL) was used with a Selemion AMV anion exchange membrane and sealed with a Kalrez Perfluoroelastomer O-ring (DuPont). Solid graphite electrodes were cut and dried at 200 °C before use. The graphite electrodes were submerged to have a surface area of (1 mm x 10 mm x 3mm). The cell was sparged for an hour with water-saturated argon and tested under an argon atmosphere. The H cell was stirred vigorously during charge-discharge measurements.

III. Solubility Studies

*Solubility of $Co_6S_8(PTA)_6$•4HCl (**1**) in water*

A 0.233 mM working stock solution of **1** (9.9 mg, 5.82 mmol) was prepared in water (25.00 mL). A quartz cell was filled with DI water (4.00 mL) and the UV-vis spectrum was recorded. The quartz cell was then spiked with the working stock solution (40 µL) six times with the UV-vis spectrum acquired after each spike at λ = 262 nm (Figure S1). A calibration curve was obtained by plotting the absorbances against concentration (Figure S2). A supersaturated solution was obtained by sonicating an excess of solid in 1 mL which was then allowed to sit overnight to equilibrate. An aliquot from the supersaturated solution (10 µL) was diluted to 25 mL and then diluted again (1 mL to 5 mL) to reach the linear range of the calibration curve.

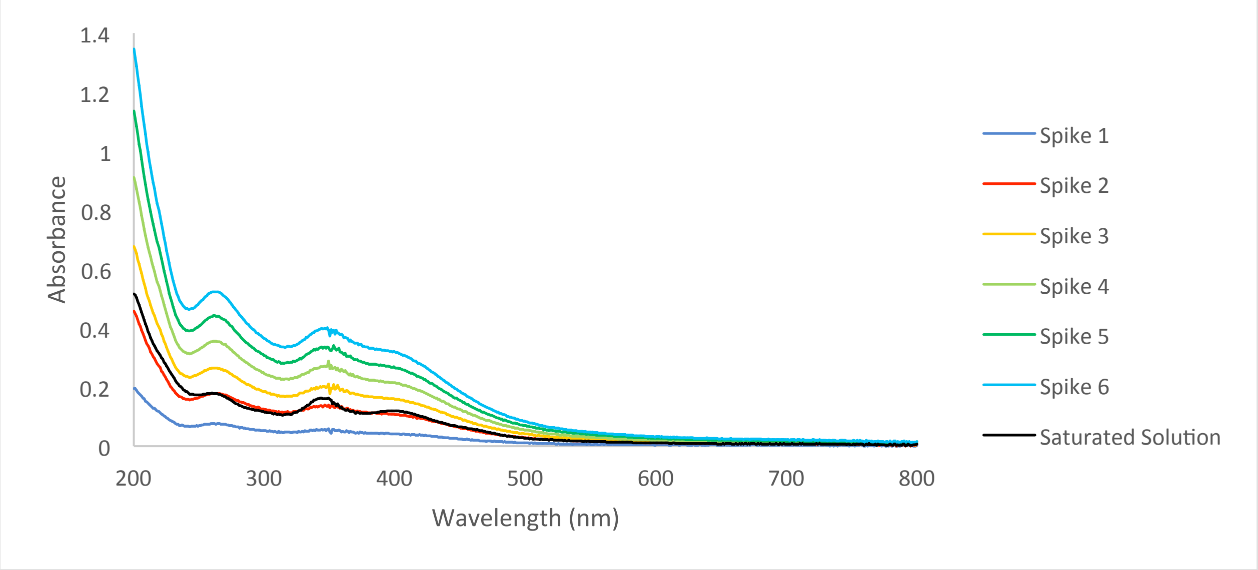

Figure S1. The overlaid absorbance spectra of $Co_6S_8(PTA)_6$•4HCl with absorbances at 262, 342, and 400 nm, respectively.

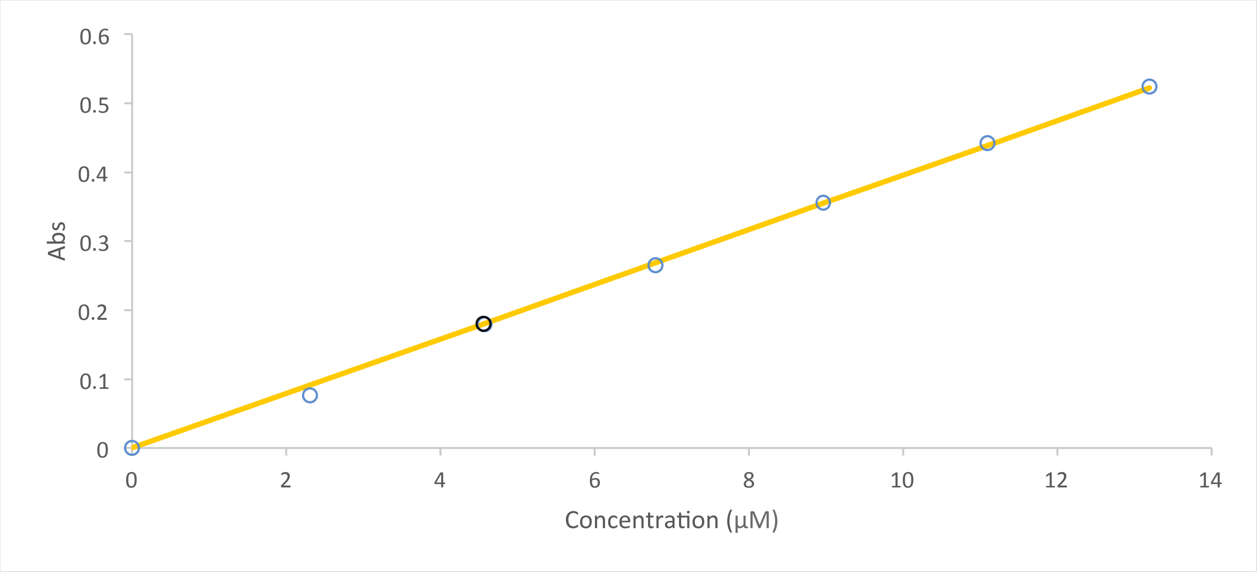

Linear Regression Equation: $y = 0.0395x$

Figure S2. Beer's Law plot of absorbance at 262 nm for **1** in water.

Absorbance of the spiked solution (blue) was plotted against concentration to give a linear calibration curve with the diluted saturated solution concentration (black) also plotted.

Spike	Abs	Concentration (µM)	Volume (mL)
0	0	0	4.000
1	0.076	2.31	4.040
2	0.179	4.57	4.080
3	0.265	6.79	4.120
4	0.355	8.96	4.160
5	0.442	11.1	4.200
6	0.524	13.2	4.240
Saturated	0.180	4.55	5.000

Calculated Saturation Point: 0.057 mM

Table S1. The absorbance data collected from the diluted solutions.

*Solubility of $Co_6S_8(PTA)_6$•4HCl (**1**) at pH 1*

A 0.257 mM working stock solution of **1** (4.36 mg, 2.57 mmol) was prepared in a solution of pH 1 with HCl (10.00 mL). A quartz cell was filled with DI water (4.00 mL) and the UV-vis spectrum was recorded. The quartz cell was then spiked with the working stock solution

(40 μL) seven times with the UV-vis spectrum acquired after each spike at λ = 338 nm (Figure S1). A calibration curve was obtained by plotting the absorbances against concentration (Figure S2). A supersaturated solution was obtained by sonicating an excess of solid in 1 mL which was then allowed to sit overnight to equilibrate. An aliquot from the supersaturated solution (5 μL) was diluted to 25 mL and then used as Unknown 1. An aliquot (2 mL) of the 25 mL solution was diluted to 4 mL and used as Unknown 2. Both unknowns fell on the linear range and the saturation point of the solution was calculated as the average.

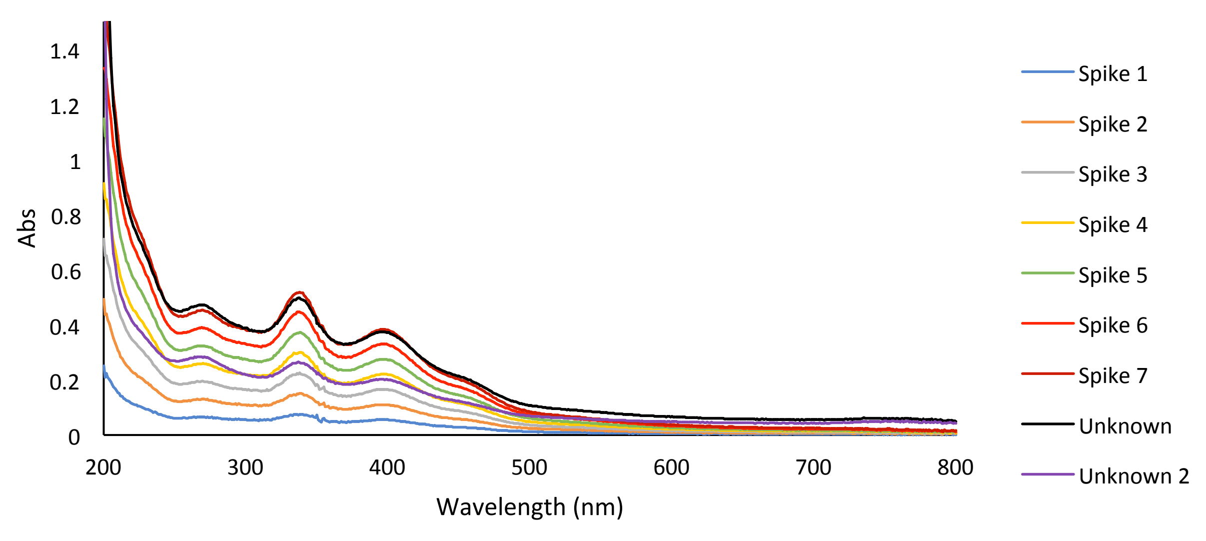

Figure S3. The overlaid absorbance spectra of $Co_6S_8(PTA)_6 \cdot 4HCl$ with absorbances at 271, 338, and 395 nm, respectively.

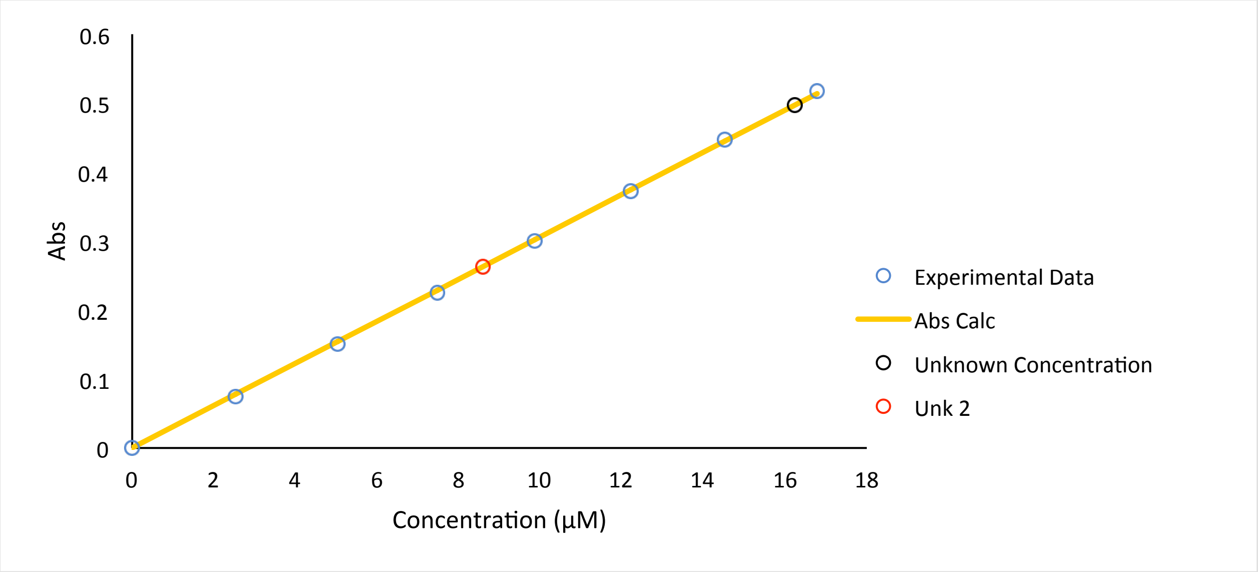

Linear Regression Equation: y = 0.0306x

Figure S4. Beer's Law plot of absorbance at 338 nm for **1** in water.

Absorbance of the spiked solution (blue) was plotted against concentration to give a linear calibration curve with the diluted saturated solution concentration (black and red) also plotted.

Spike	Abs	Concentration (µM)	Volume (mL)
0	0	0	4.000
1	0.075	2.54	4.040
2	0.150	5.03	4.080
3	0.225	7.47	4.120
4	0.300	9.87	4.160
5	0.373	12.2	4.200
6	0.447	14.5	4.240
7	0.518	16.8	4.280
Unk 1	0.497	16.2	25.000
Unk 2	0.263	8.59	4.000

Calculated Saturation Point: 0.084 mM

Table S2. The absorbance data collected from the diluted solutions.

IV. NMR Spectroscopy

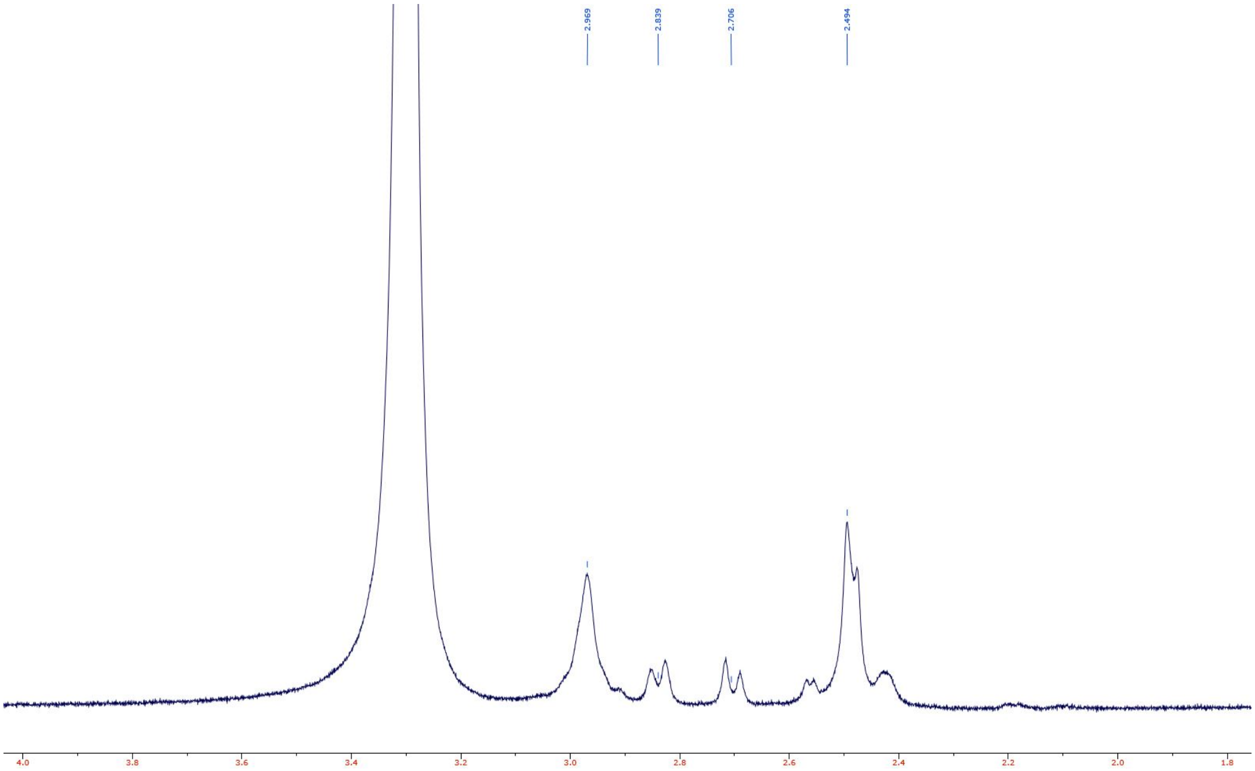

Figure S5. WATERGATE ^{1}H NMR spectrum of **1** (D_2O, 500 MHz, 25 ^oC).

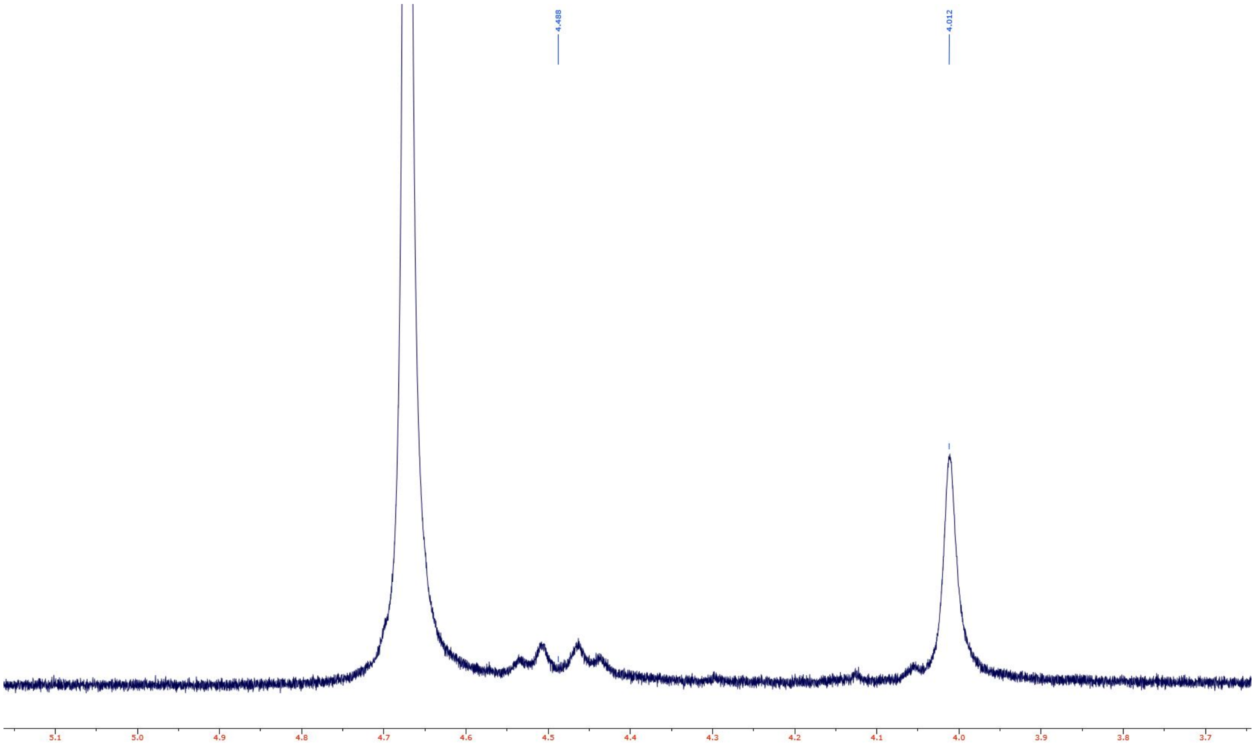

Figure S6. WATERGATE ^{1}H NMR spectrum of **1** after deprotonation with K_2CO_3 (D_2O, 500 MHz, 25 ^{o}C).

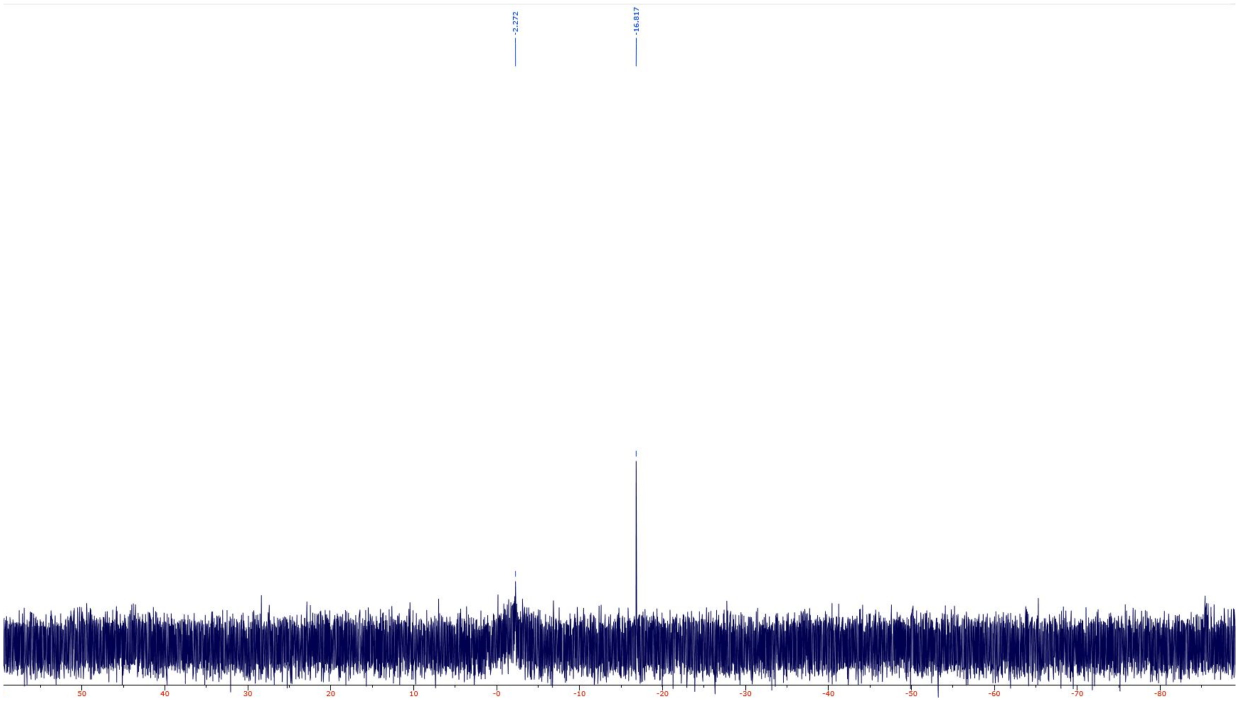

Figure S7. The ^{31}P NMR of 1 (D_2O, 500 MHz, 25 ^{o}C).

Evans Method

A concentrated solution of **1** was made using a standard solution of 35% DCl in D_2O. A sealed capillary of the pure 35% DCl solution was added to the NMR tube and the spectrum was ran. Only one DCl signal was observed.

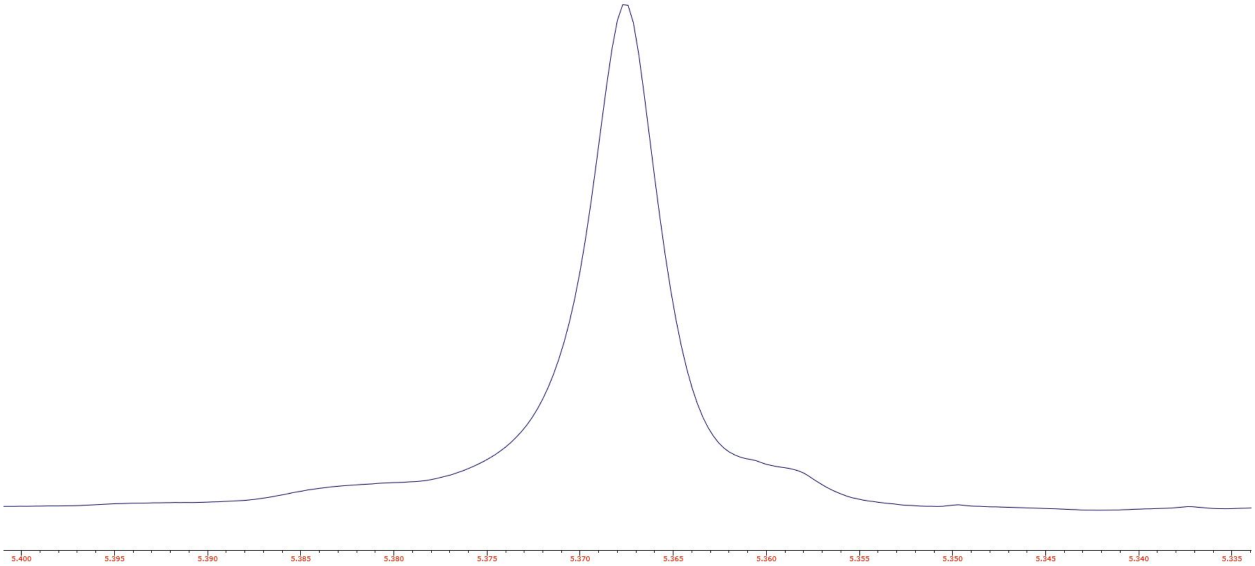

Figure S8. ^1H NMR solvent peak of **1** (35% DCl in D_2O, 300 MHz, 25 ^oC) with a capillary of pure DCl solution sealed within the NMR tube.

V. X-ray Diffraction

Data were collected on an Agilent Gemini Diffractometer equipped with a CCD area detector and operated at 40 kV, 40 mA to generate Mo Kα radiation (λ = 0.71073 Å). The incident X-ray beam was focused and monochromated. The crystal was mounted on a nylon loop with Parabar grease frozen by low temperature N_2 flow. Neither cracking nor crystal decay was ever encountered under this condition. An initial scan was taken to gain preliminary unit cell parameters and to assess the mosaicity of the crystal to select the required frame width for data collection. Frame widths were set at 0.5° for data collection. Following data collection, reflections were sampled from all regions to re-determine unit cell parameters for data integration. Absorption correction was performed after the data integration by the program SADABS.[2] Initial scan images of the crystals clearly revealed dense diffraction patterns, which indicated a large unit cell. The structure was solved by direct methods and refined using the Olex 2 (version 1.2.8) software suite.[3] Atoms were located from iterative examination of difference F-maps following least squares refinements of an earlier model. The final model was refined anisotropically until full convergence was achieved. For the UNCC_Co6S8_PTA crystal, 100K was found to be optimum for data collection. All atoms were unambiguously determined with chemically reasonable bond lengths and bond angles. C-H hydrogen atoms were placed in calculated positions (Distance C-H: 0.93 Å) and included as riding atoms with isotropic displacement parameters 1.2 times Ueq of the attached C atoms. The hydrogen atom involved in hydrogen bonding between the PTA nitrogen N23 and the chloride ion was located in a difference map and refined isotropically. Because of the very limited free space in between the densely packed clusters, the SQUEEZE program was not applied.

A dark crimson black needle crystal was glued on a nylon tip with P grease and flash frozen to 100 K in a liquid N_2 cooled stream of N_2. Parameters of the x-ray diffractometer were set as described. A total of 10020 reflections were collected, of which 2694 were unique. The range of θ was from 3.29° to 25.00°. The structure was solved in the orthorhombic space group Cmca, with Z = 4, using direct methods. Atoms were identified by obtaining chemically logical bond lengths and angles, and by identifying peaks from subsequent difference electron density maps corresponding to six-membered rings of the TPA ligand. All the non-hydrogen atoms were refined anisotropically, with hydrogen atoms generated as spheres riding the coordinates of their parent C atoms. The hydrogen atom involved in N-Cl hydrogen bonding was refined isotropically as described above. Final full matrix least-squares refinement on F^2 converged to R1 = 0.0489 (F >2σ(F)) and wR2 = 0.1040 (all data) with GOF = 1.059.

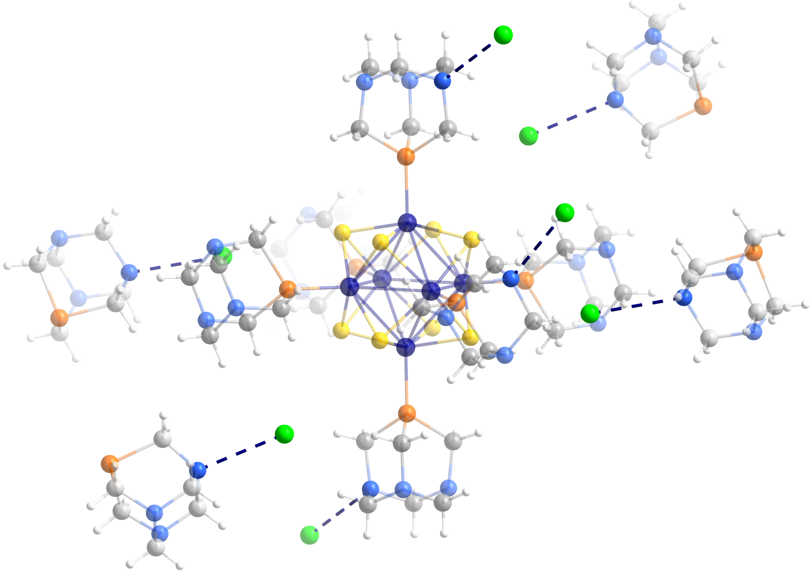

Figure S9. Ball-and-stick X-ray crystal structure of $Co_6S_8(PTA)_6•4HCl$ (**1**) as viewed from the side illustrating the hydrogen bonding interaction between PTA nitrogen and chloride. Carbon, grey; chlorine, green; cobalt, dark blue; hydrogen, white; nitrogen, light blue; phosphorus, orange; sulfur, yellow.

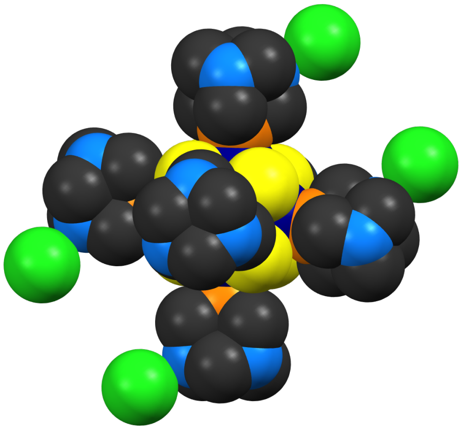

Figure S10. Space filling X-ray crystal structure of $Co_6S_8(PTA)_6•4HCl$ (**1**) as viewed from the side. Carbon, grey; chlorine, green; cobalt, dark blue; nitrogen, light blue; phosphorus, orange; sulfur, yellow.

Table S3. Crystal Data of UNCC_Co6S8_PTA6

Identification code	UNCC_Co6S8_PTA6
Empirical formula	$C_{36} H_{76} Cl_4 Co_6 N_{18} P_6 S_8$
Formula weight	1698.84
Temperature/K	100(2)
Crystal system	orthorhombic
Space group	Cmca
a/Å	23.1218(19)
b/Å	10.7247(9)
c/Å	24.0502(17)
α/°	90
β/°	90
γ/°	90
Volume/Å^3	5963.8(8)
Z	4
ρcalc g/cm^3	1.892
μ/mm^{-1}	2.301
F(000)	3464
Crystal size/mm^3	0.1 × 0.05 × 0.02
Radiation	Mo Kα (λ = 0.71073 Å)
2Θ range for data collection/°	6.58 to 50
Index ranges	$-29 \leq h \leq 21$, $-9 \leq k \leq 14$, $-31 \leq l \leq 31$
Reflections collected	10020
Independent reflections	2694 [Rint = 0.0733, Rsigma = 0.0932]
Data/restraints/parameters	2694/0/191
Goodness-of-fit on F^2	1.059
Final R indexes [I>=2σ (I)]	R1 = 0.0489, wR2 = 0.1040
Final R indexes [all data]	R1 = 0.0749, wR2 = 0.1136
Largest diff. peak/hole / e Å^{-3}	0.84/-0.68

VI. Cyclic Voltammetry

*Diffusion Coefficient*s

A BASi glassy electrode (GC) working electrode (WE) was polished with alumina on a felt surface and the had its area standardized by chronoamperometry by using the known diffusion coefficient of K3Fe(CN)6 following conditions from previously reported literature.4 The same electrodes were rinsed and then used at varying scan rates (ν) in a solution of 1 (1 mM) with NaCl (0.5 M) as the supporting electrolyte. The same method was applied while studying 1 (1 mM) with HCl (1.0 M) as the supporting electrolyte. By applying the Randles-Sevcik equation (1), the diffusion coefficient (D) of 1 was found at room temperature (T) for both the mono (water and acid) and dicationic species (water only).

$$(1) \qquad i_p = 0.4463nFAC\left(\frac{nF\nu D}{RT}\right)^{1/2}$$

For Equation 1, i_p is the forward peak current, n is the number of electrons transferred, F is Faradays constant, C is the bulk concentration of the active species, R is the universal gas constant, and A is the area of the electrode.

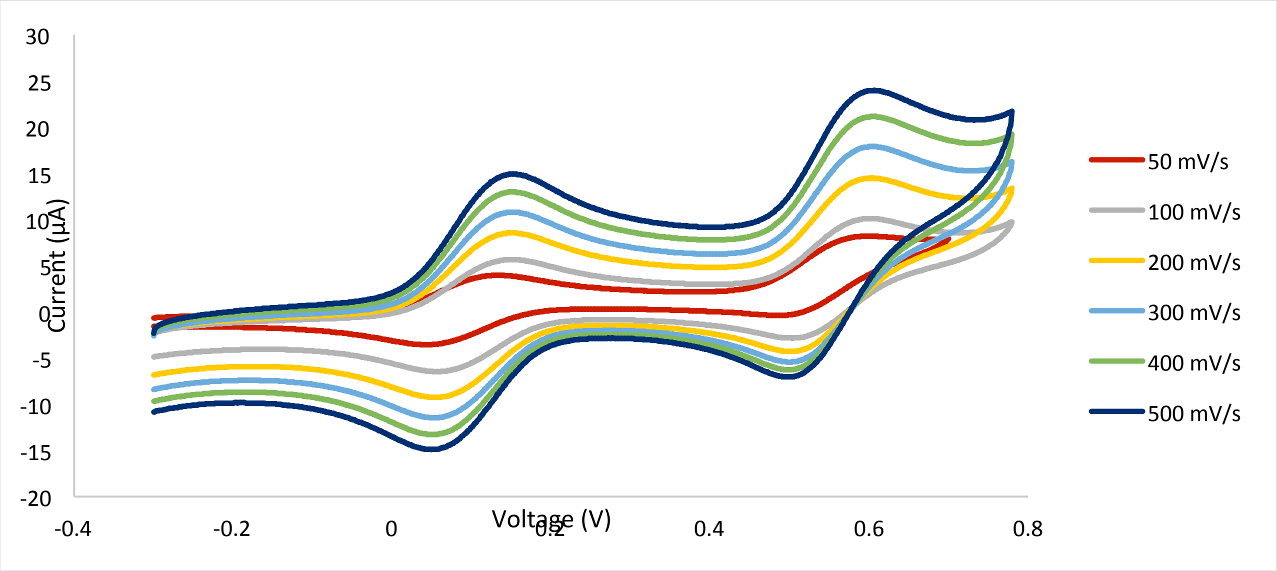

Figure S11. Cyclic voltammograms of **1** (1 mM, 0.5 M NaCl, H_2O) at various scan rates were taken on a GC WE at 20.5 °C and referenced versus Ag/AgCl.

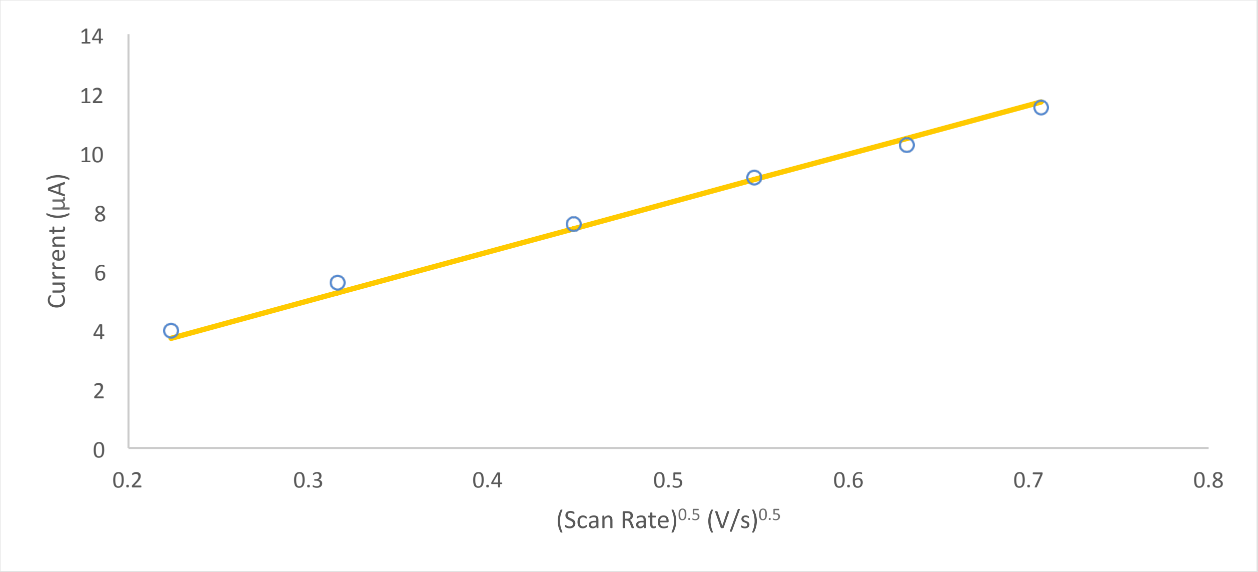

Figure S12. The plot of current as a function of the square root of the scan rate for the monocation of **1** in water.

$D = 6.9*10^{-7}$ cm^2/s

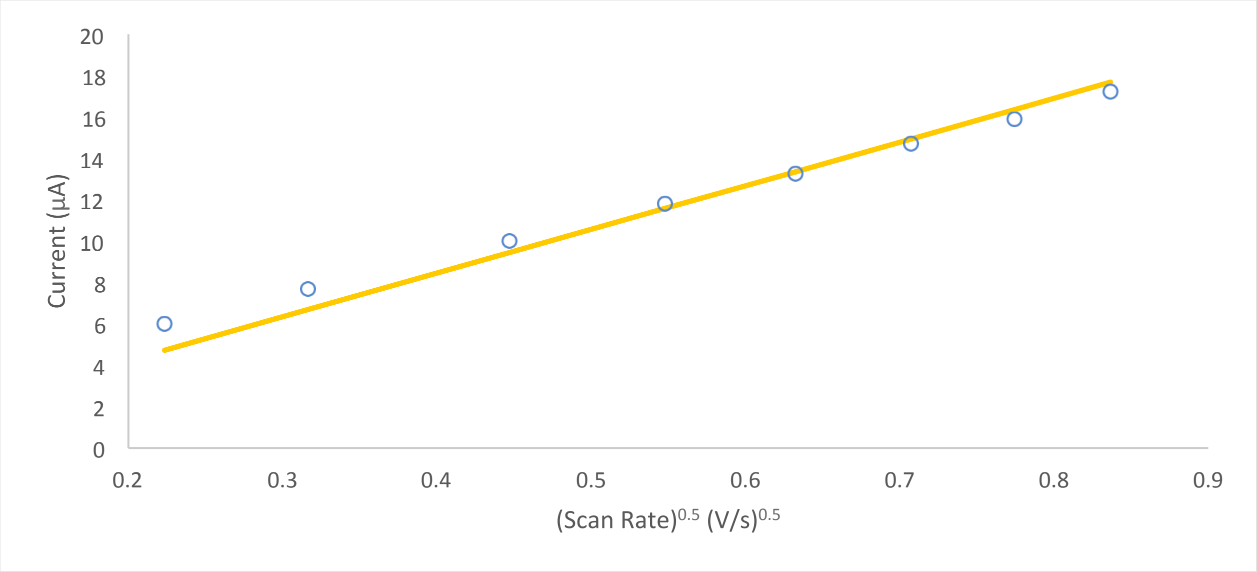

Figure S13. The plot of current as a function of the square root of the scan rate for the dication of **1** at in water.

D = 1.12*10^{-6} cm^{2}/s

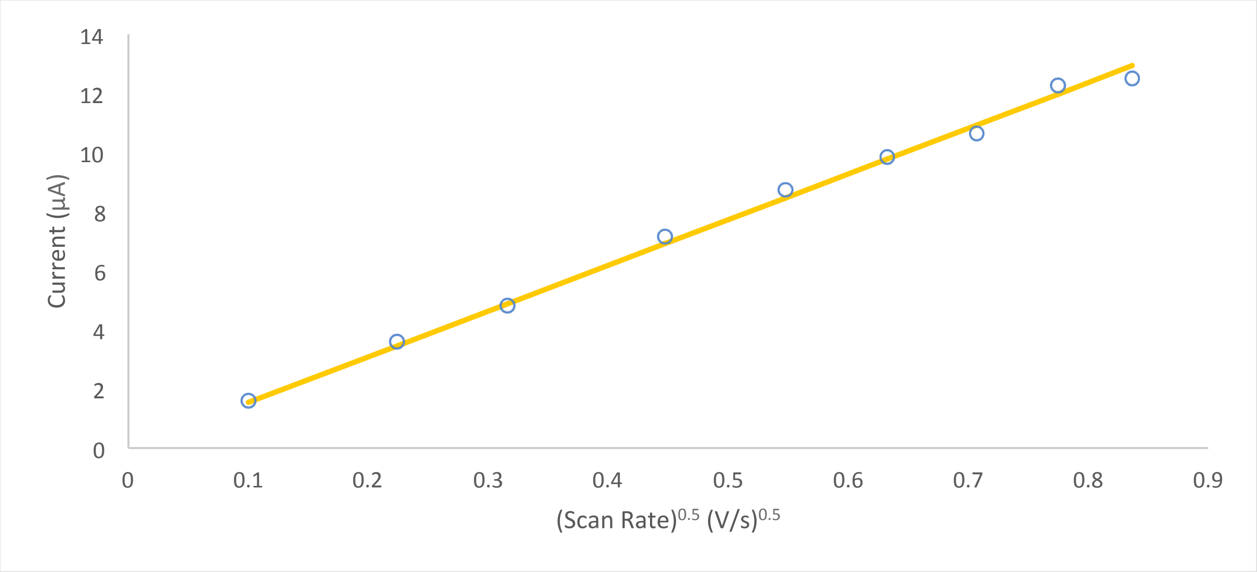

Figure S14. The plot of current as a function of the square root of the scan rate for the monocation of **1** at pH 0.

D = 5.48*10^{-7} cm^{2}/s

Electron Transfer Coefficients

A BASi glassy electrode (GC) working electrode (WE) was polished with alumina on a felt surface. The scan rates were varied in a solution of **1** (1 mM) with NaCl (0.5 M) as the supporting electrolyte. The same method was applied while studying **1** (1 mM) with HCl (1.0 M) as the supporting electrolyte. The peak separation (ΔE_p) was measured as a function of scan rate and then used to find the dimensionless rate parameter (ψ) using the Nicholson method[5] assuming α = 0.5. Using Equation 2, the electron transfer rate coefficient (k^0) was calculated by plotting the ψ as a function of the inverse square root of the scan rate ($\nu^{-1/2}$).

$$\psi = \frac{k^0}{\left(\frac{\pi D F \nu}{RT}\right)^{1/2}} \qquad (2)$$

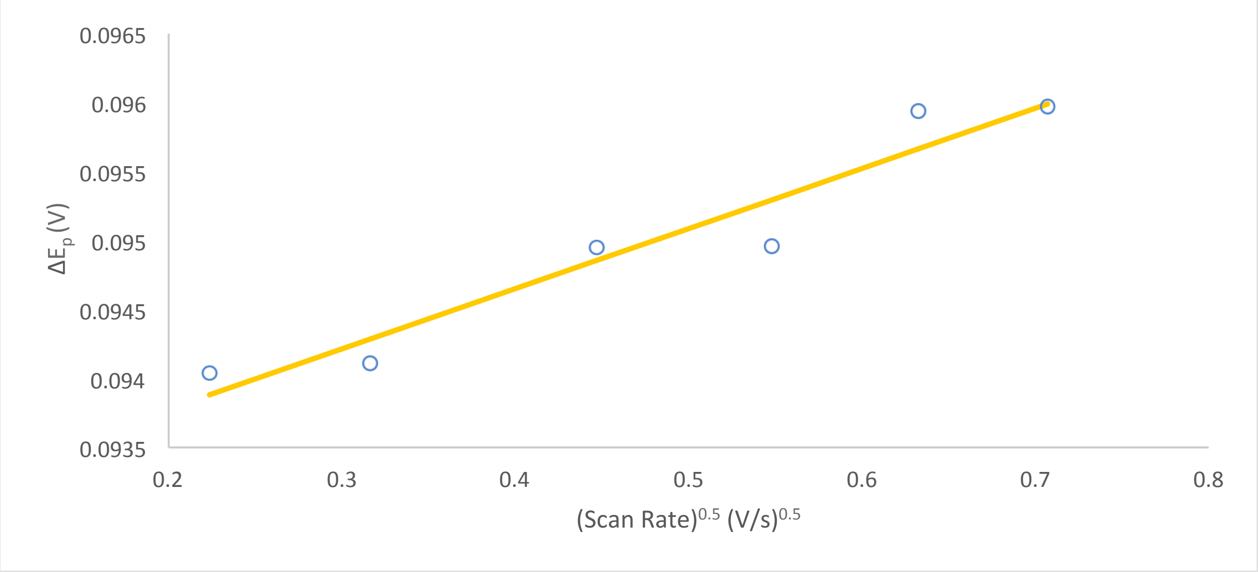

$k^0 = 2.22 * 10^{-3}$ cm/s

Figure S15. An aqueous solution of **1** (1 mM) supported by NaCl (0.5 M) with the peak separation plotted as a function of the square root of the scan rate.

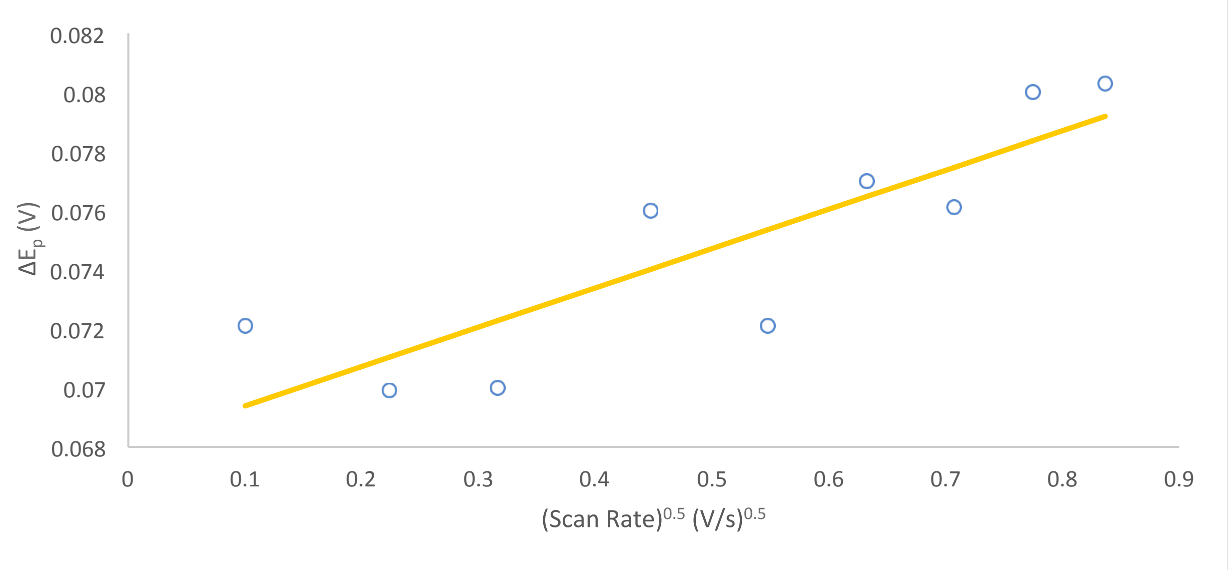

$k^0 = 7.45*10^{-3}$ cm/s

Figure S16. An aqueous solution of **1** (1 mM) supported by HCl (1.0 M) with the peak separation plotted as a function of the square root of the scan rate.

Solution Stability

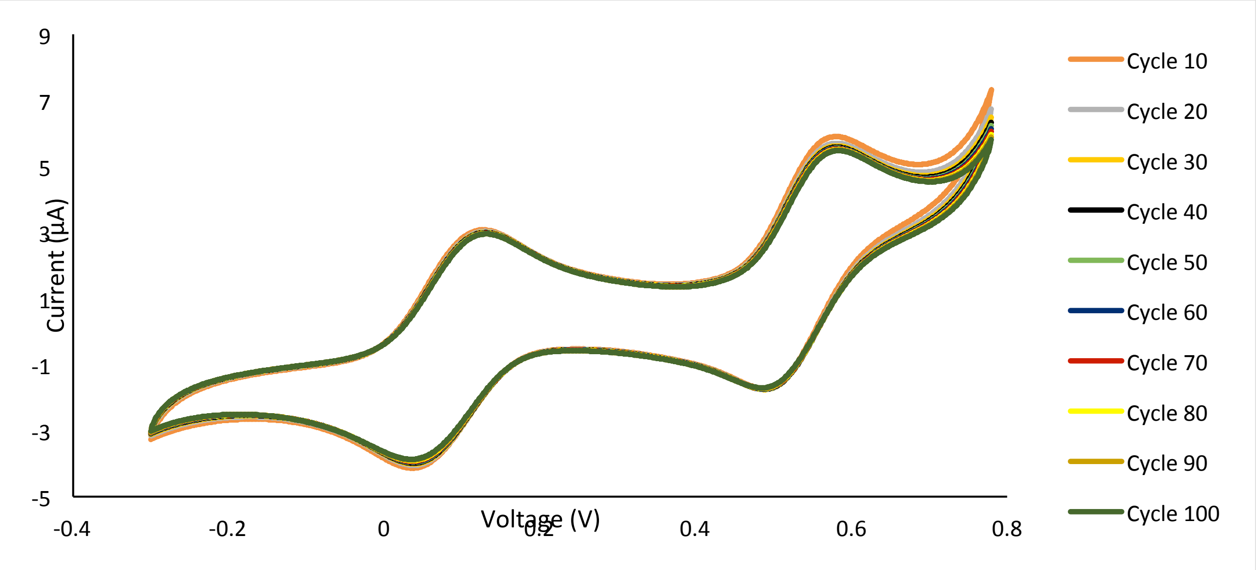

Figure S17. Overlay of CVs of **1** in aqueous NaCl cycled 100 times at 50 mV/s on a GC WE and referenced versus Ag/AgCl.

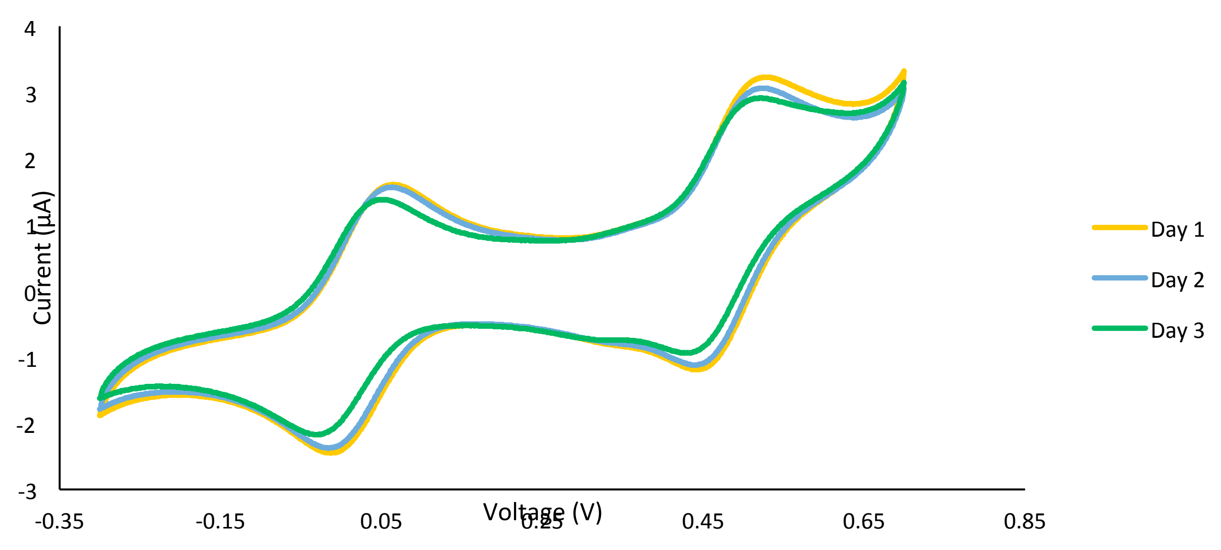

Figure S18. Overlay of CVs of **1** in aqueous NaCl using a GC WE at 100 mV/s and referenced versus Ag/AgCl. Solutions were left open to air for 3 days.

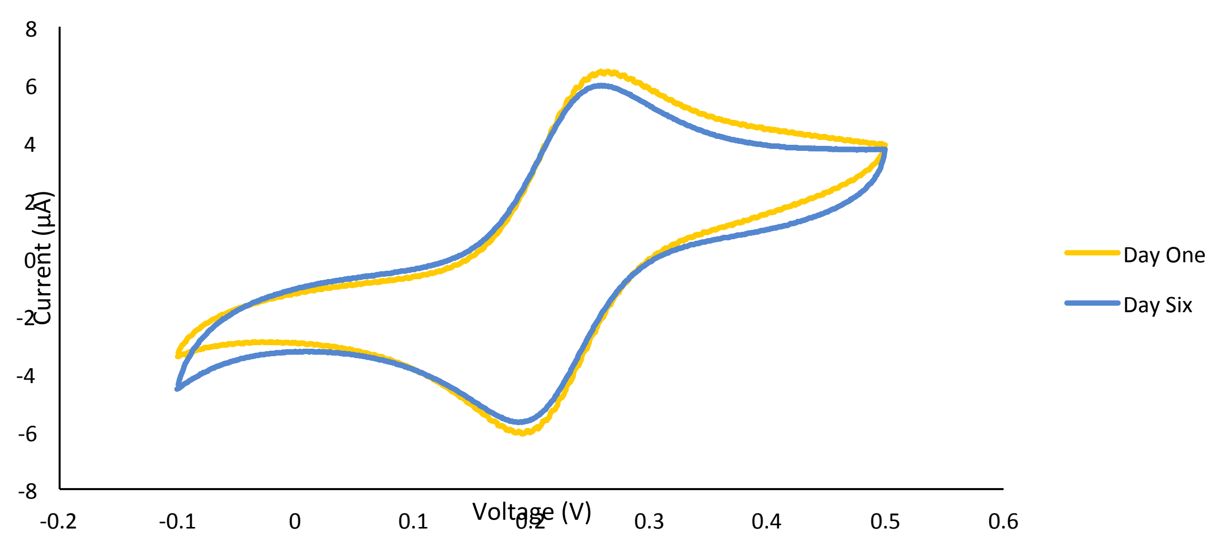

Figure S19. Cyclic voltammogram of **1** (1 mM, 1 M HCl, H_2O) at 100 mv/S referenced versus Ag/AgCl.

Cyclic Voltammogram – pH Studies

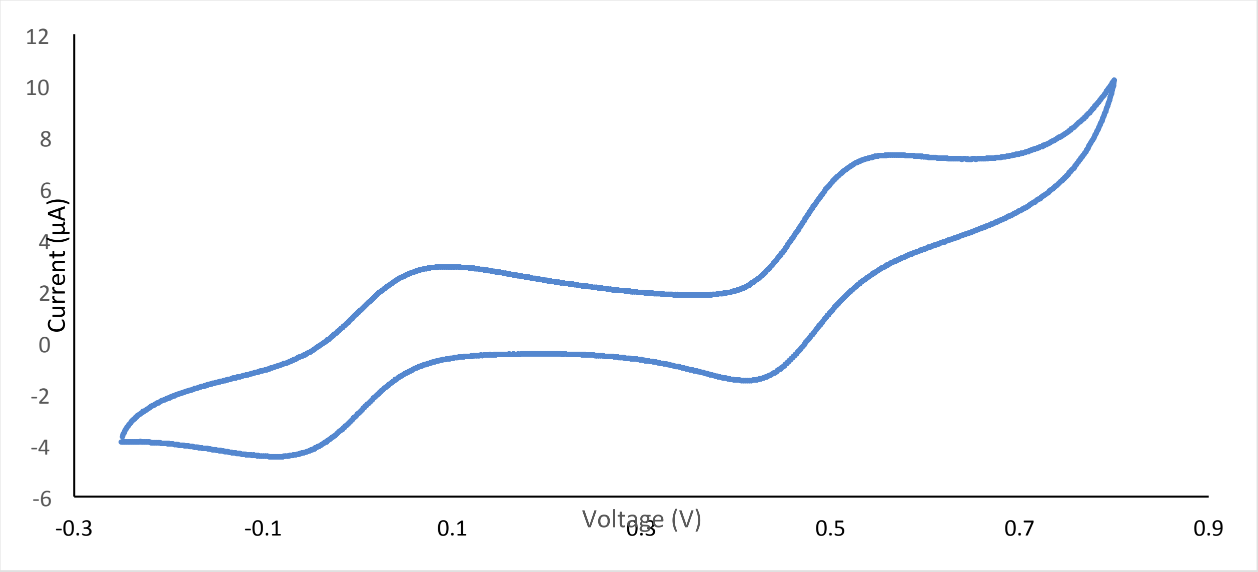

Figure S20. CV of **1** (1 mM) in a citric acid and sodium phosphate dibasic buffer at pH 7 recorded with a GC WE at 100 mV/s and referenced versus Ag/AgCl.

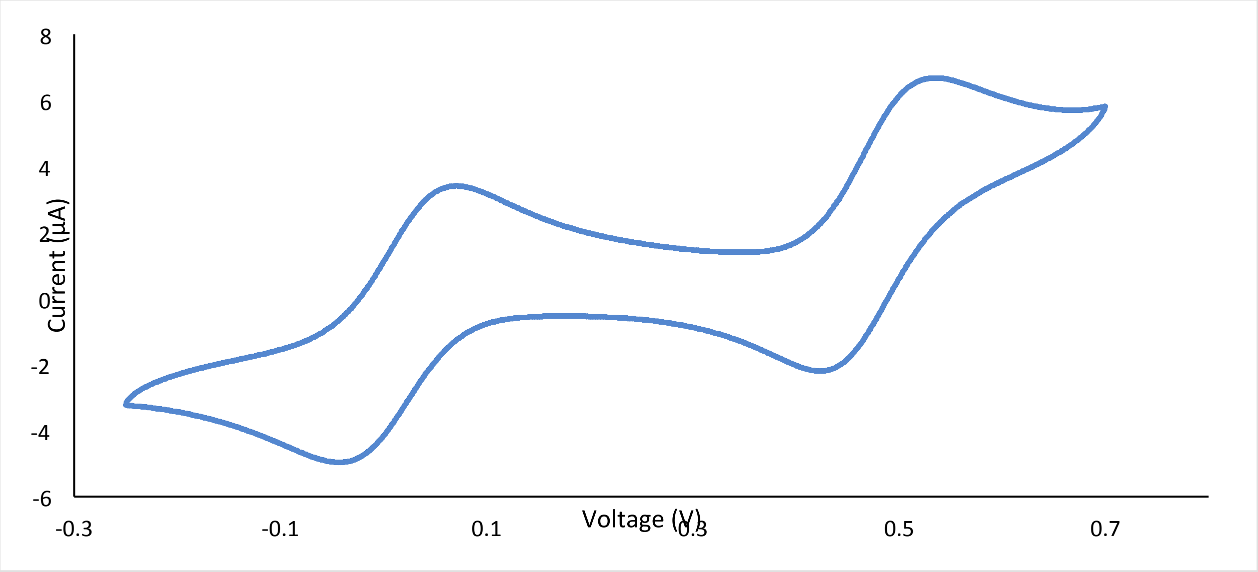

Figure S21. CV of **1** (1 mM) in a citric acid and sodium phosphate dibasic buffer at pH 6 recorded with a GC WE at 100 mV/s and referenced versus Ag/AgCl.

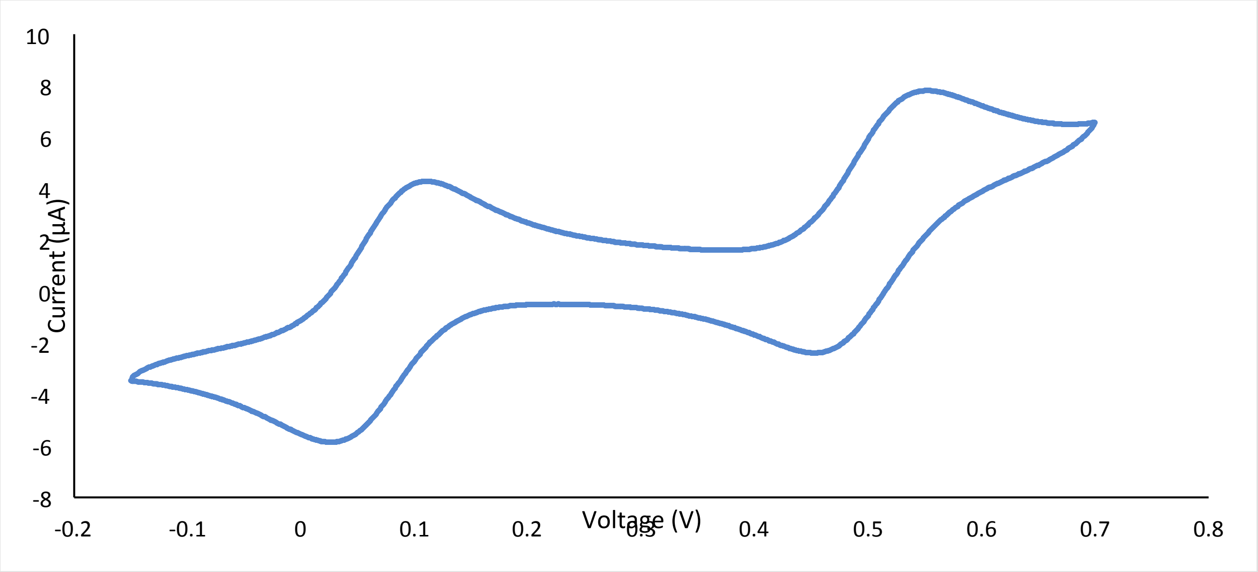

Figure S22. CV of **1** (1 mM) in a citric acid and sodium phosphate dibasic buffer at pH 5 recorded with a GC WE at 100 mV/s and referenced versus Ag/AgCl.

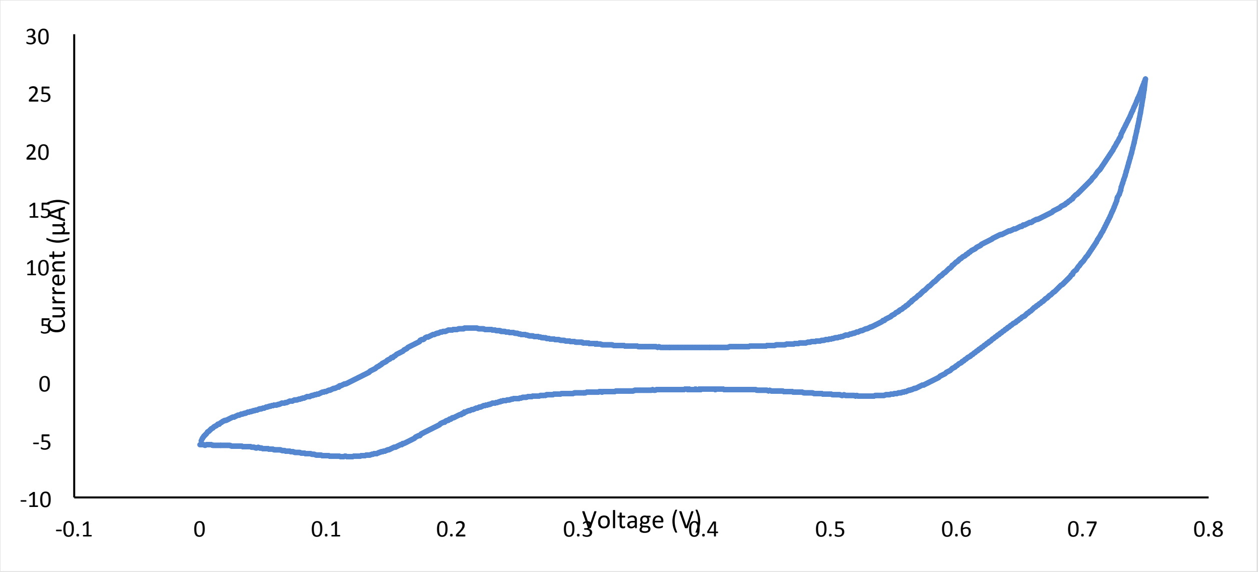

Figure S23. CV of **1** (1 mM) in a citric acid and sodium phosphate dibasic buffer at pH 4 recorded with a GC WE at 100 mV/s and referenced versus Ag/AgCl.

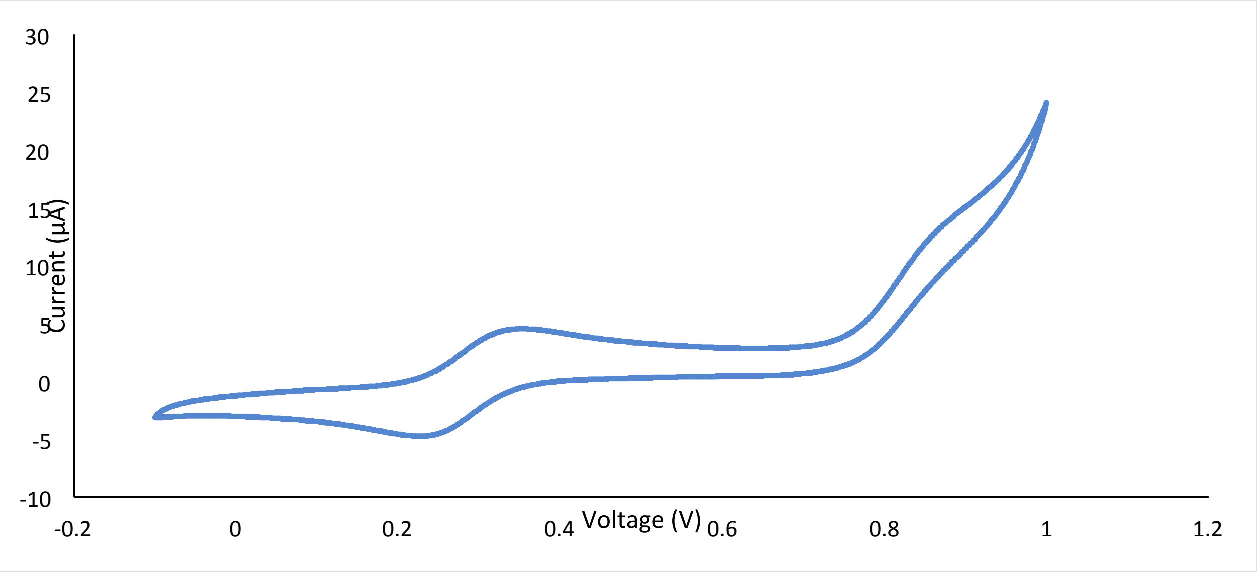

Figure S24. CV of **1** (1 mM) acidified to pH 1 with HCl recorded with a GC WE at 100 mV/s and referenced versus Ag/AgCl.

pH	$E_{1/2}$ (V)
7	0
6	0.01
5	0.07
4	0.16
1	0.29

Table S4. The $E_{1/2}$ values of the **1**/**1**$^+$ redox event tabulated as a function of pH.

VII. Galvanostatic Charge-Discharge Experiments

Half Cell Experiments

A 1 mM aqueous stock solution (10 mL) of **1** (17.1 mg, 10 mmol) with NaCl (0.5846 g, 10.0 mmol) was made. The stock solution of **1** (4 mL) was pipetted into each side of the H-cell. The theoretical capacity (C_p) was calculated to find the capacity at an 80% state of charge (SOC) using Equation 2 based on solution volume (V), concentration (C), number of electrons transferred (n), and Faradays constant (F).

(3) $$C_p = \frac{1000VCnF}{3600}$$

Theoretical Capacity:

-From Co_6S_8 to $Co_6S_8^{1+}$

$$Cp = \frac{\left(1000\ \frac{mA}{A}\right) * (0.004\ L) * (0.001\ M) * (1\ e^{-}) * \left(96485 \frac{C}{mol}\right)}{3600\ \frac{s}{h}}$$

$$C_p = 0.107\ mAh$$

$$80\%\ SOC = 0.085\ mAh$$

Set Experimental Parameters:

Charging current was set to 28.5 µA for 3 h and the discharging current was set for 21 µA for 4 h with cut off voltages at 0.12 and -0.1 V, respectively.

-From Co_6S_8 to $Co_6S_8^{2+}$

$$Cp = \frac{\left(1000\ \frac{mA}{A}\right) * (0.004\ L) * (0.001\ M) * (2\ e^{-}) * \left(96485 \frac{C}{mol}\right)}{3600\ \frac{s}{h}}$$

$$C_p = 0.214\ mAh$$

$$80\%\ SOC = 0.171\ mAh$$

Set Experimental Parameters:

Charging current was set to 85.6 µA for 2 h and the discharging current was set for 43 µA for 3 h with cut off voltages at 0.7 and -0.25 V, respectively.

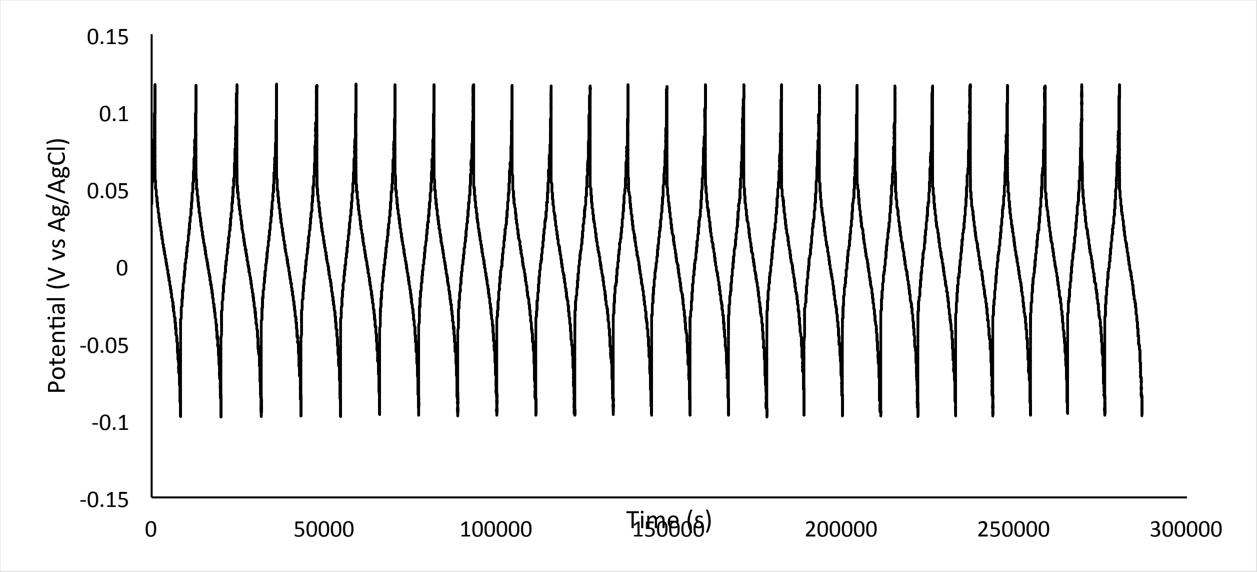

Figure S25. Galvanostatic cycling of 4 mL of **1** (1 mM, 1 M NaCl, H_2O) with a charging current of 29 µA and a discharge current of 21 µA to 80% state of charge with voltage referenced versus Ag/AgCl .

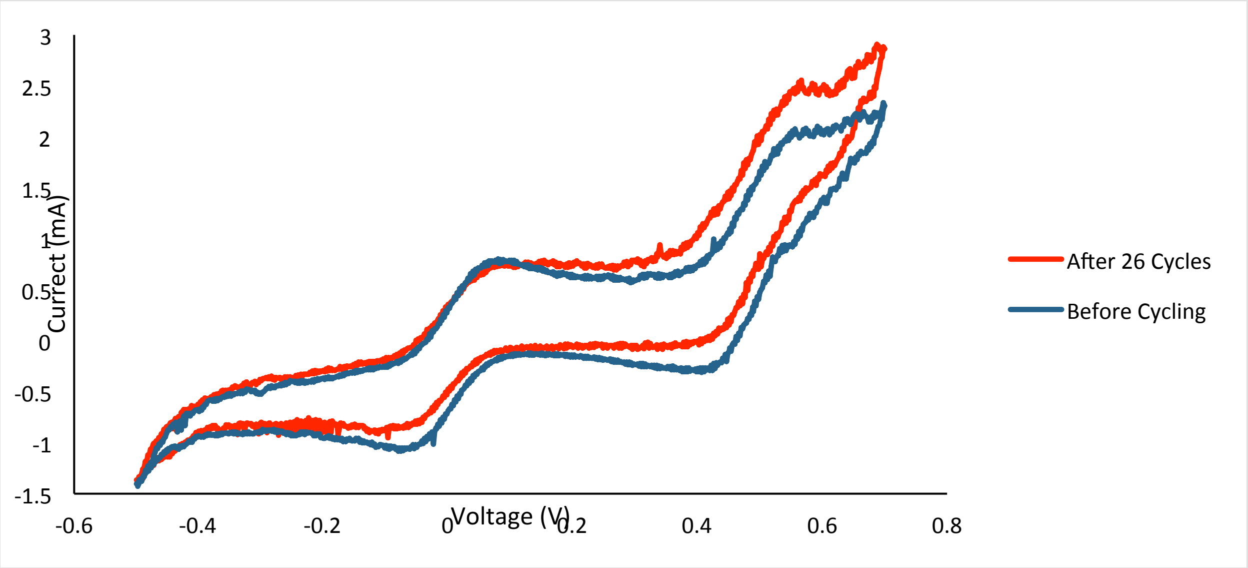

Figure S26. Cyclic voltammogram of **1** (1 mM, 1 M NaCl, H_2O) before and after 26 cycles taken in the H-cell with a graphite felt working electrode and referenced versus Ag/AgCl.

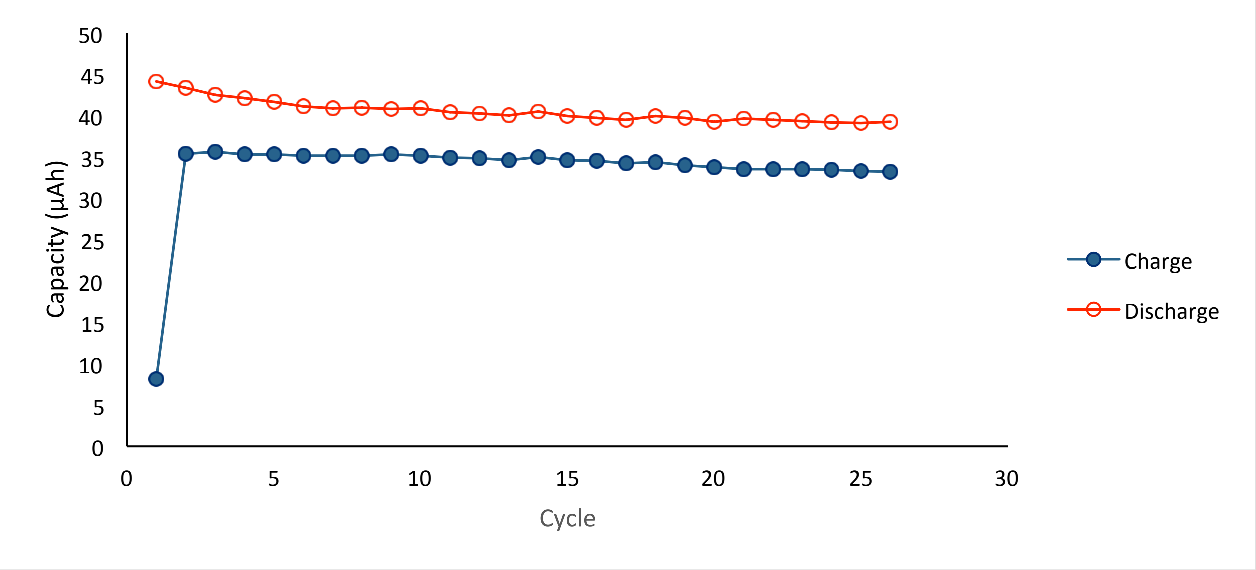

Figure S27. Plot of capacity charged and discharged for 26 cycles for 1e$^-$ cycling of **1**/**1**$^+$ (1mM) in a H cell supported by 1 M NaCl.

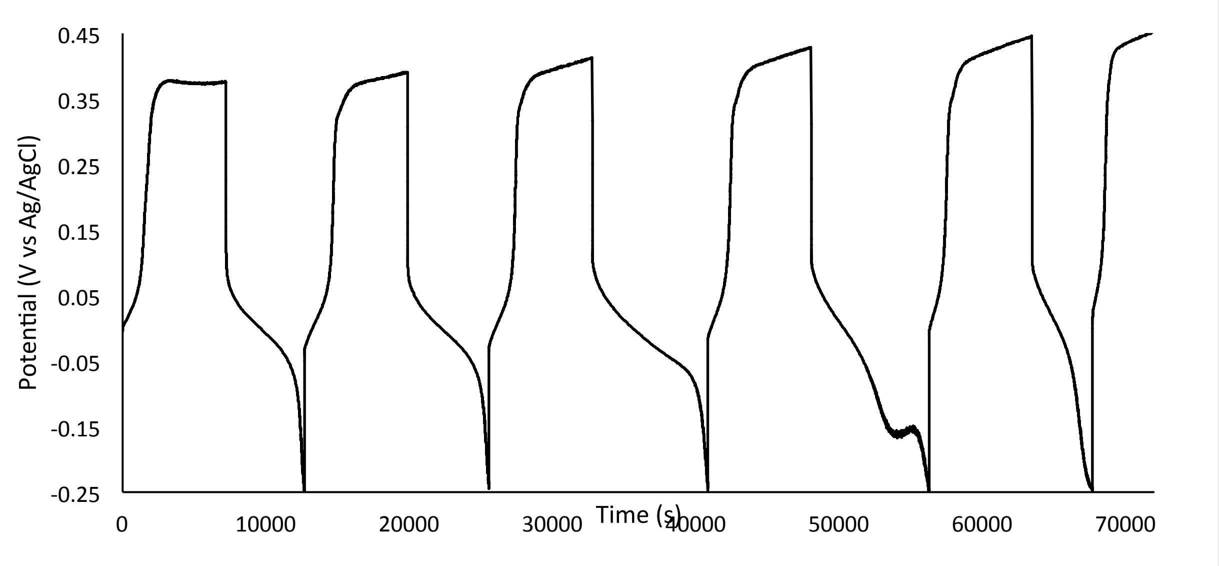

Figure S28. Galvanostatic cycling of 4 mL of **1** (1 mM, 1 M NaCl, H_2O) with a charging current of 85 µA and a discharge current of 43 µA to 80% state of charge with voltage referenced versus Ag/AgCl .

Full Cell Experiment

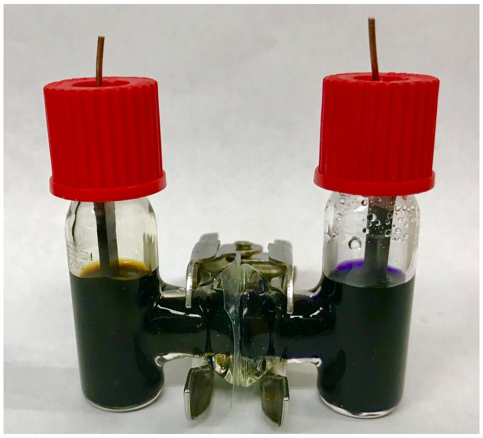

Figure S29. H cell with cluster **1** on the left (brown), methyl viologen (MV) on the right (purple), a Selemion AMV anion exchange membrane in the center, two graphite plates connected with copper wire and a 5mM NaCl supporting electrolyte. The image was taken after a charging cycle and consists of $\mathbf{1}^+$ and $MV^{\bullet +}$.

A 2.5 mM aqueous solution (25 mL) of methyl viologen hydrate (17.2 mg $MV^{2+}\bullet H_2O$, 62.5 µmol) used as the cell anolyte. The anolyte (5 mL) consisted of NaCl (0.2922 g, 5.0 mmol) and the methyl viologen solution. The cathylote is a 2.5 mM aqueous solution (5 mL) of **1** (21.2 mg, 12.5 µmol) and NaCl (0.2922 g, 5.0 mmol). The H Cell was assembled in atmosphere with 4 mL of the anolyte and catholyte added to each side and was sparged with water-saturated argon for one hour before cycling experiments. The cell was tested at 80% SOC.

Set Experimental Parameters:

Charging current was set to 107 µA for 2 h and the discharging current was set to 71 µA for 3 h with cut off voltages at 0.1 and 1.2 V, respectively. The theoretical capacity is 0.268 mAh with a capacity of 0.214 mAh at 80% SOC.

VIII. Cost Estimation

Preliminary cost estimations were calculated using the bulk material prices (Alibaba.com) in order to approximate the preparative synthetic cost of **1** on an industrial scale. This calculation was based on recently reported RFB cost approximations by Friedl and coworkers,[6] which used bulk elemental prices, and is modified here to account for costs of industrial staring materials. The synthetic costs of tetrakis(hydroxymethyl)phosphonium chloride (TCP-Cl), 1,3,5-Triaza-7-phosphaadamantane (PTA), and cluster **1** were individually calculated (Table S5). Methanol solvent was not included in calculation of the total preparative cost. A quantitative yield for each step was assumed in all calculations. The total cost for synthesis of cluster **1** is estimated at $2.78/kg and $4.73/mol.

Compound[a]	MW	Equiv	mol	$/g	Amount (g)	$	Intermediate
PH_3	33.99	1	1	0.01	33.99	0.34	THPCl
HCl	36.46	1	1	0.003	36.46	0.11	
Formaldehyde[b]	30.02	4	4	0.0004	120.10	0.13	
NaOH	39.99	1	1	0.0002	39.99	0.008	PTA
Methenamine	140.19	1	1	0.0008	140.19	0.12	
Formaldehyde[b]	30.02	1	1	0.0004	30.02	0.03	
$CoCl_2 \bullet 6H_2O$	273.91	1	1	0.005	273.91	1.37	Cluster (**1**)
H_2S	34.08	1.33	1.33	0.012	45.44	0.54	

[a] All compounds were sourced in bulk from Alibaba.com

[b] Based on a 37% Formalin solution with d = 1.083.

Table S5. Preliminary cost analysis for preparation of **1**.

IX. References

1 F. Joó, J. Kovács, Á. Kathó, A. C.Bényei, T. Decuir and D. J. Dubois, *Inorganic Syntheses*, John Wiley & Sons, Inc., Hoboken, NJ, USA, 1996, vol. 32.

2 L. Krause, R. Herbst-Irmer, G. M. Sheldrick and D. Stalke, *J. Appl. Crystallogr.*, 2015, **48**, 3–10.

3 O. V. Dolomanov, L. J. Bourhis, R. J. Gildea, J. A. K. Howard and H. J. Puschmann, *J. Appl. Crystallogr.*, 2009, **42**, 339–341.

4 S. J. Konopka and B. McDuffie, *Anal. Chem.*, 1970, **42**, 1741–1746.

5 R. S. Nicholson, *Anal. Chem.*, 1965, **37**, 1351–1355.

6 J. Friedl, M. A. Lebedeva, K. Porfyrakis, U. Stimming and T. W. Chamberlain, *J. Am. Chem. Soc.*, 2018, **140**, 401–405.